believed to be the primary method of vessel formation in gliomas. Angiogenesis requires three distinct steps: (1) blood vessel breakdown, (2) degradation of the vessel basement membrane and surrounding ECM, and (3) migration of endothelial cells and the formation of new blood vessels.[49]

Blood vessel breakdown

The first step of angiogenesis is the dissolution of native vessels aspects. Glioma cells first accumulate around the existing cerebral blood vessels and lift off the astrocytic foot processes, which leads to the disruption of the normal contact between endothelial cells and the basement membrane.[66] The affected endothelial cells express angiopoietin-2 (Ang-2) resulting in destabilization of the vessel wall and decreased pericyte coverage.[26,66,68] Ang-1 and -2 are important endothelial growth factors that signal via the Tie2 receptor tyrosine kinase (RTK) expressed on endothelial cells. In the normal brain, Ang-1 binds to Tie2, inducing association between pericytes and endothelial cells and resulting in stabilization of the vasculature.[6,55] Conversely, Ang-2 may act as an antagonist to Tie2 phosphorylation, and lead to destabilization of blood vessels. Therefore, Ang-2 represents a checkpoint for Ang-1/Tie2-mediated angiogenesis.[44,66]

Degradation of the vessel basement membrane and surrounding ECM

Degradation of the vessel basement membrane and surrounding ECM facilitates the invasion of endothelial cells. This step is an integral part of the ongoing angiogenic process.[56] Gelatinase-A (MMP-2) and gelatinase-B (MMP-9) are highly expressed in astrocytomas.[21,52] MMP-2 and MMP-9 expression is strongly induced by hypoxia, and these two molecules appear to have a synergistic effect on basement membrane degradation.[36]

Migration of endothelial cells and formation of new blood vessels

After regression of existing vessels and breakdown of the basement membrane, endothelial cells proliferate and migrate toward the tumor cells expressing pro-angiogenic compounds. Integrin $\alpha v\beta 3$ and $\alpha 5\beta 1$ are upregulated in endothelial cells during angiogenesis, enhancing endothelial cell adhesion and migration.[10,32] Migration of pericytes is an important part of tumor vessel formation. Platelet-derived growth factor (PDGF) that is secreted by activated endothelial cells recruits pericytes to the site of newly sprouting vessels and aids in establishing a new basement membrane.[20,41]

Molecular Biology of GBM Invasion

One of the insidious biological features of gliomas is the potential of single cells to invade normal brain tissue. Details of the glioma invasion mechanisms are only beginning to be determined.

Tumor cell invasion requires four distinct steps: (1) detachment of invading cells from the primary tumor mass, (2) adhesion to ECM, (3) degradation of ECM, and (4) cell motility and contractility.[49]

Detachment of invading cells from the primary tumor mass

The detachment of invading glioma cells from the primary tumor mass involves several events. The first event is destabilization and disorganization of cadherin-mediated junctions that hold the primary mass together. The second event is a decline in the expression of connexin 43. The reduction in connexion 43 leads to the reduction in gap junction formation.[23] The third event is cleavage of CD44. CD44 anchors the primary mass to ECM, by the metalloproteinase A Disintegrin and Metalloproteinase (ADAM).[48]

Adhesion to ECM

Integrins are the most common molecules that allow glioma cells to adhere to ECM. In particular, the integrin $\alpha v\beta 3$ is thought to play a central role in glioma invasion. Integrin $\alpha v\beta 3$ binds to fibronectin, vitronectin, and tenascin-C in ECM.[39]

ECM degradation

MMPs are the most common proteases that degrade the ECM and create space for the invading glioma cells. MMP-2 and MMP-3 levels and MMP-2/MMP-9 activity correlate with glioma cell migration and invasion.[64]

Cell motility and contractility

Cell motility requires cytoplasmic contractile force. Myosin II allows glioma cells to squeeze through pores smaller than their nuclear diameter, which is important because the brain has particularly narrow extracellular spaces.[3] Small GTPases, such as RhoA, Rac, cdc42, as well as RLC-interacting protein are also involved in this process in glioma cells.[7,57]

Animal Models for Studying Glioma Invasion and Angiogenesis

Studying glioma invasion and angiogenesis are challenging, because most animal models fail to mimic the unique features of human glioma cell invasiveness and angiogenesis[16]. Typically, such transplantable tumors in mice or rats form solid

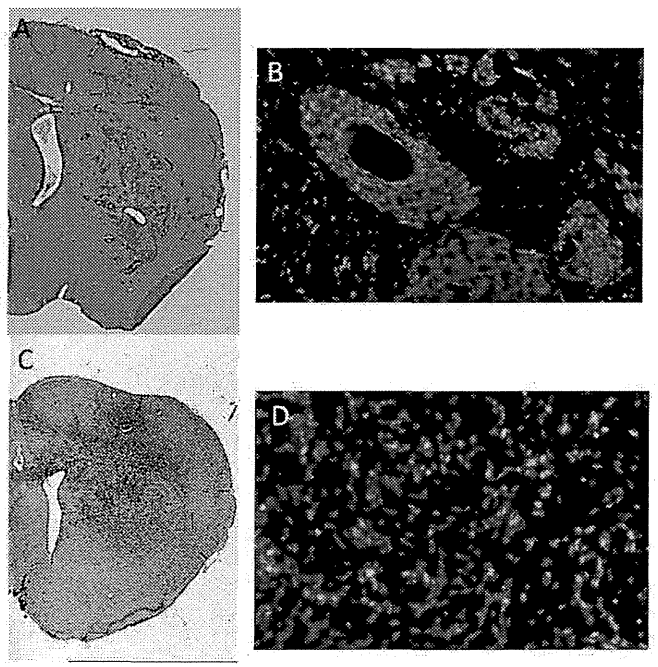

Fig. 2 Two distinct invasion phenotypes in animals harboring J3T-1 and J3T-2 brain tumors. A, B: A J3T-1 brain tumor was established in athymic rat brains. C, D: J3T-1 cells formed well demarcated and highly angiogenic tumors in the rat brain. Multiple small satellite tumors are also seen at tumor borders. A J3T-2 brain tumor was established in athymic rat brains. J3T-2 cells gradually dispersed from the tumor center to the surrounding normal brain tissue. A and C: hematoxylin-eosin staining. B and D: vascular stain (RECA-1, red) and nuclear stain (DAPI, blue). DAPI: 4',6-diamidino-2-phenylindole, RECA: rat endothelial cell antigen.

nodules at the injection site and compress rather than invade the surrounding brain regions.

We have established two novel animal models with different invasive and angiogenic phenotypes. Two subclones, J3T-1 and J3T-2, were established by passage of the parental canine glioma cell line, J3T, in immunocompromised animals. These cells established tumors following intracerebral inoculation in athymic mouse and rat.[27] J3T-1 cells clustered around dilated blood vessels at tumor borders whereas J3T-2 cells showed diffuse single cell infiltration into surrounding normal parenchyma. Marked angiogenesis was seen only in J3T-1 gliomas (Fig. 2). The described animal models histologically imitated two invasive and angiogenic phenotypes, namely angiogenesis-dependent and -independent invasion, which is also observed in human GBM. Angiogenesis-dependent invasion is that tumor cells coopt around pre-existing vessels and secrete angiogenic factors to develop neovasculature and tumor cells proliferate around newly developed vessels and migrate along them, resulting in the formation of perivascular cuffing. Angiogenesis-independent invasion is that tumor cells migrate as single cells along myelinated axons without inducing angiogenesis. These novel models would be particularly beneficial for analyzing the molecular mechanisms of glioma invasion and angiogenesis and investigating new glioma therapies.[27,46,49,50] We performed proteomic analysis using J3T-1 (angiogenesis-dependent invasion phenotype) and J3T-2 (angiogenesis-independent invasion phenotype) to investigate the molecular basis of invasion and angiogenesis by malignant gliomas.[46] One of the proteins identified was annexin A2, which was expressed at higher levels in J3T-1 than in J3T-2. Moreover, immunohistochemical analysis of human GBM specimens showed that annexin A2 was expressed at high levels in the tumor cells that formed clusters around dilated vessels. Thus, annexin A2 may be related to angiogenesis-dependent invasion.[46]

Bevacizumab

Bevacizumab (Avastin) is a recombinant humanized monoclonal antibody that targets VEGF; it was the first anti-angiogenesis agent to be approved by the United States Food and Drug Administration (FDA) in 2004. Several Phase II clinical trials have studied the therapeutic efficacy of bevacizumab as a single-agent

or in combination with chemotherapy or radiation for recurrent GBM. The results support the conclusion that bevasizumab is effective for recurrent GBM. Bevacizumab has demonstrated encouraging radiographic response in patients with recurrent malignant gliomas.[58] Retrospective studies have also supported the same conclusion.[2,14] In 2013, during the American Society of Clinical Oncology (ASCO) Annual Meeting, the results of the positive phase III AVAglio study was presented by Roger Henriksson et al.[25] The study showed bevacizumab in combination with radiation and temozolomide chemotherapy reduced the risk of cancer progression or death (progression-free survival; PFS) by 36% in people with newly diagnosed GBM. The results for overall survival (OS) did not reach statistical significance. The result of the phase III RTOG 0825 study was presented at the 2013 ASNO Annual Meeting by Gilbert et al. The RTOG 0825 study was the double-blind placebo-controlled trial evaluating bevacizumab in patients with newly diagnosed GBM. The addition of bevacizumab for newly diagnosed GBM did not improve OS, but improved PFS, but did not reach the significance criterion. De Groot et al.[15] showed that patients with glioma developed an apparent phenotypic shift to a predominantly infiltrative pattern of tumor progression after treatment with bevacizumab. Indeed, a preclinical study showed that anti-angiogenic therapy of murine gliomas with an antibody against VEGF-R2 caused small satellite tumors to arise near the primary mass, centered around core vessels, which is similar to the perivascular invasion found more recently in the VEGF knockout glioma cell lines that were described previously.[37] Further research is needed to identify mediators of this invasion and to determine whether the invasion seen after bevacizumab treatment of human GBM is the perivascular invasion seen in the murine cell lines or the parenchymal type of invasion along white matter typically seen in GBM.[4] It has been proposed that hypoxia caused by vessel regression during the course of anti-angiogenic therapy leads to up-regulation of proangiogenic factors and recruitment of bone marrow-derived cells (BMDCs) that have the capacity to increase tumor growth by means of new blood vessel growth.[5] Glioma cells evade antiangiogenic therapies by up-regulating alternative proangiogenic signal circuits, including those utilizing fibroblast growth factor, ephrin A1, and angiopoietin 1. Another adaptive measure is the hypoxia-regulated recruitment of vascular progenitor cells and proangiogenic monocytes from the bone marrow to tumors.[5]

Cilengitide

Cilengitide (EMD121974), an inhibitor of αvβ3 and αvβ5 integrins, demonstrated preclinical efficacy against malignant glioma.[43] It is speculated that cilengitide can inhibit tumor growth, invasion, and angiogenesis. However, the effects of cilengitide on these processes have not been sufficiently examined.

We investigated the anti-glioma effect of cilengitide using DNA microarray analysis. U87ΔEGFR cells (human malignant glioma cell line) were used for this experiment. The cells were harvested after 16 h of cilengitide treatment, and mRNA was extracted. Gene expression and pathway analyses were performed using a DNA microarray (CodeLink™ human whole Genome Bioarray, [Applied Microarrays, Inc., Tempe, AZ, USA]). The expression of 264 genes was changed with cilengitide treatment. The expression of 214 genes was up-regulated and that of 50 genes was down-regulated compared to the controls. In pathway analysis, "apoptotic cleavage of cellular proteins" and "TNF receptor signaling pathway" were over-represented. Apoptotic-associated genes such as caspase 8 were up-regulated. We revealed that cilengitide activated caspase-8 and induced apoptosis-related pathways (Fig. 3).[51]

In our previous study, we investigated the anti-glioma mechanisms of cilengitide utilizing the novel invasive glioma models, J3T-1 (angiogenesis-dependent invasion phenotype) and J3T-2 (angiogenesis-independent invasion phenotype). Cilengitide treatment resulted in a significantly decreased diameter of the J3T-1 tumor vessel clusters and its core vessels when compared to controls, while an anti-invasive effect was shown in the J3T-2 brain tumor with a significant reduction of diffuse cell infiltration around the tumor center (Fig. 4). Our results indicate that cilengitide exerts a phenotypic anti-tumor effect by inhibiting angiogenesis and glioma cell invasion in vivo.[50] Angiogenesis requires three distinct steps: (1) blood vessel breakdown, (2) degradation of the vessel basement membrane and surrounding ECM, and (3) migration of endothelial cells and the formation of new blood vessels.[60] During the third step of angiogenesis, integrin αvβ3 is upregulated in endothelial cells, enhancing endothelial cell adhesion and migration.[10,11] The final product of glioma angiogenesis is a vasculature with highly tortuous dilated vessels.[60] Cilengitide prevents the third step of angiogenesis and reduces the size of tumor vessels. Glioma cell invasion requires four distinct steps: (1) detachment of invading cells from the primary tumor mass, (2) adhesion to the ECM, (3) degradation of the ECM, and (4) cell motility and contractility.[49] Integrins are the molecules that allow glioma cells to adhere to the ECM during the second step.[60] Cilengitide might inhibit the second step, thereby suppressing the invasion of glioma.

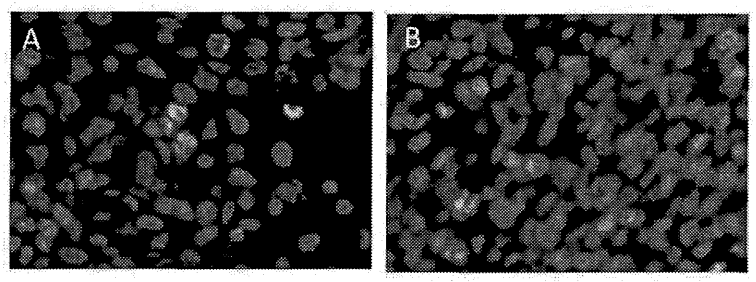

Fig. 3 In vivo immunohistochemical analysis of caspase 8 expression in U87ΔEGFR brain tumors. U87ΔEGFR cells were injected into the right frontal lobe of athymic rats. Cilengitide or phosphate buffered saline (PBS) was administered 3 times/week intraperitoneally starting on day 5 after tumor cell implantation. To assess the expression of caspase 8, athymic rats harboring U87ΔEGFR brain tumors were sacrificed at 14 days after tumor implantation. A subpopulation of caspase 8-positive cells was visualized using immunostaining (caspase 8-positive cells: caspase 8, red; nuclei: DAPI, blue) of U87ΔEGFR control xenografts (A) and U87ΔEGFR cilengitide-treated xenografts (B). The control sections exhibited scattered red fluorescence (A), whereas more punctate red fluorescence was observed in the cilengitide-treated xenografts (B). DAPI: 4',6-diamidino-2-phenylindole.

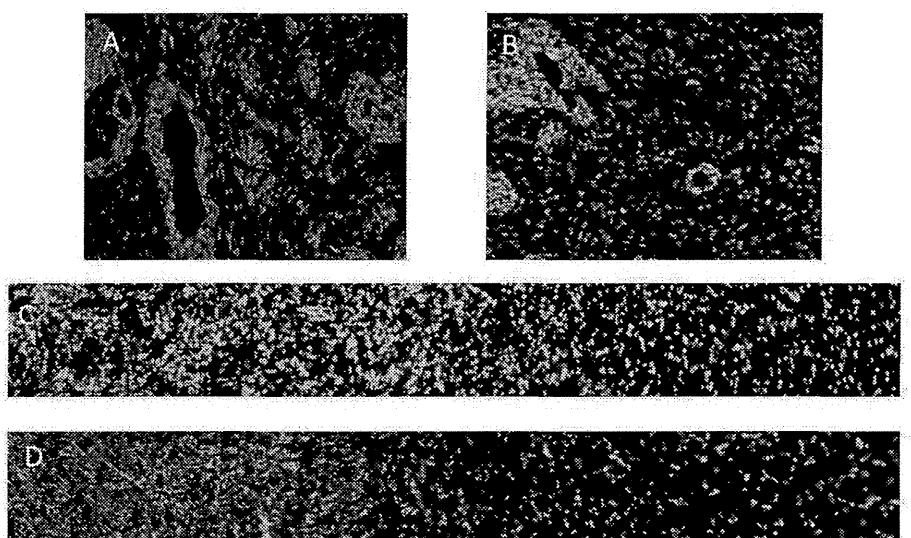

Fig. 4 Bimodal anti-glioma mechanisms of cilengitide demonstrated by novel invasive glioma models. Anti-angiogenic effects of cilengitide on the J3T-1 brain tumor in rats. Examined with immunofluorescence staining (vascular: RECA-1, red; nuclei: DAPI, blue), the diameter of the J3T-1 tumor clusters' core vessels in cilengitide-treated animals (B) was smaller than that in untreated animals (A). We observed the anti-invasive effects of cilengitide on the J3T-2 gliomas in rats. Immunofluorescence staining (vascular endothelial cells: RECA-1, red; nuclei: DAPI, blue) of J3T-2 control tumors (C) and cilengitide-treated J3T-2 tumors (D) revealed that the tumor borders in treated animals were more evident. The cell density of control tumors was gradually reduced from the tumor center toward the normal brain parenchyma, while the cell density of treated tumors dropped steeply at the tumor border.DAPI: 4',6-diamidino-2-phenylindole, RECA: rat endothelial cell antigen.

Several preclinical studies have shown an enhanced antitumor effect of cilengitide when administered in combination therapeutic regimens.[1,12,53,61] Mikkelsen et al. demonstrated that cilengitide dramatically amplified the efficacy of radiation therapy in an animal glioma model.[47] We demonstrated the enhanced therapeutic efficacy of an oncolytic virus on experimental glioma following pretreatment with cilengitide.[35] This research showed that pretreatment of gliomas with the angiogenesis inhibitor cilengitide reduced inflammation, vascular hyperpermeability, and leukocyte infiltration of tumor tissue upon

treatment with oncolytic virus. Reduction of host immune responses by cilengitide treatment enhanced the anticancer efficacy of oncolytic virus treatment by increasing oncolytic virus propagation in tumors. We also reported that oncolytic HSV-1 infection of tumors induces angiogenesis and upregulates cysteine-rich protein 61 (CYR61).[34] CYR61 was identified as a member of the CCN (CYR61/CTGF/NOV) family of matricelluar proteins regulating cell growth, differentiation, survival, angiogenesis, and migration in development, tissue remodeling, and repair.[38]

In order to test the role of CYR61-mediated integrin activation in Oncolytic Virus (OV)-induced angiogenesis, the impact of cilengitide on OV treatment-induced angiogenesis was investigated.[33,38]

Clinical Trials

A phase I clinical trial of cilengitide in recurrent malignant gliomas by the New Approaches to Brain Tumor Therapy (NABTT) has been completed with no dose limiting toxicities.[18] The most notable trial to date was a randomized phase II study of cilengitide, which was associated with a median survival of 10 months in recurrent glioma patients.[53] The North American Brain Tumor Consortium (NABTC) study[22] was designed to determine whether cilengitide effectively penetrates into GBM in human patients. This study confirmed that cilengitide is effectively delivered into primary human GBM tumors with good retention. The result of the CENTRIC study (phase III), which compares the efficacy and tolerability of cilengitide in patients with newly diagnosed GBM and a methylated O6-methylguanine-DNA methyltransferase (MGMT) gene promoter status,[59] was presented at 2013 ASCO Annual Meeting by Roger Stupp et al.[59] Cilengitide failed to prolong PFS or OS in patients with newly diagnosed GBM and methylated MGMT gene promoter. The previously reported safety profile of cilengitide in addition to standard therapy was confirmed. The phase II CORE trial, which included only patients with an unmethylated MGMT gene promoter status, are currently ongoing.

Conclusions

A better understanding of the molecular components responsible for glioma angiogenesis and invasion will hopefully lead to the development of new treatment methods. Antiangiogenic therapy is dramatically altering the treatment landscape for patients with GBM.

Conflicts of Interest Disclosure

The authors have no personal, financial, or institutional interest in any of the drugs, materials, or devices in the article. All authors who are members of The Japan Neurosurgical Society (JNS) have registered online Self-reported COI Disclosure Statement Forms through the website for JNS members.

References

1) Abdollahi A, Griggs DW, Zieher H, Roth A, Lipson KE, Saffrich R, Gröne HJ, Hallahan DE, Reisfeld RA, Debus J, Niethammer AG, Huber PE: Inhibition of alpha(v)beta3 integrin survival signaling enhances antiangiogenic and antitumor effects of radiotherapy. *Clin Cancer Res* 11: 6270–6279, 2005
2) Agha CA, Ibrahim S, Hassan A, Elias DA, Fathallah-Shaykh HM: Bevacizumab is active as a single agent against recurrent malignant gliomas. *Anticancer Res* 30: 609–611, 2010
3) Beadle C, Assanah MC, Monzo P, Vallee R, Rosenfeld SS, Canoll P: The role of myosin II in glioma invasion of the brain. *Mol Biol Cell* 19: 3357–3368, 2008
4) Bello L, Giussani C, Carrabba G, Pluderi M, Costa F, Bikfalvi A: Angiogenesis and invasion in gliomas. *Cancer Treat Res* 117: 263–284, 2004
5) Bergers G, Hanahan D: Modes of resistance to anti-angiogenic therapy. *Nat Rev Cancer* 8: 592–603, 2008
6) Bergers G, Song S: The role of pericytes in blood-vessel formation and maintenance. *Neuro-oncology* 7: 452–464, 2005
7) Bornhauser BC, Lindholm D: MSAP enhances migration of C6 glioma cells through phosphorylation of the myosin regulatory light chain. *Cell Mol Life Sci* 62: 1260–1266, 2005
8) Brahimi-Horn C, Berra E, Pouysségur J: Hypoxia: the tumor's gateway to progression along the angiogenic pathway. *Trends Cell Biol* 11: S32–36, 2001
9) Brem S, Cotran R, Folkman J: Tumor angiogenesis: a quantitative method for histologic grading. *J Natl Cancer Inst* 48: 347–356, 1972
10) Brooks PC, Clark RA, Cheresh DA: Requirement of vascular integrin alpha v beta 3 for angiogenesis. *Science* 264: 569–571, 1994
11) Brooks PC, Montgomery AM, Rosenfeld M, Reisfeld RA, Hu T, Klier G, Cheresh DA: Integrin alpha v beta 3 antagonists promote tumor regression by inducing apoptosis of angiogenic blood vessels. *Cell* 79: 1157–1164, 1994
12) Burke PA, DeNardo SJ, Miers LA, Lamborn KR, Matzku S, DeNardo GL: Cilengitide targeting of alpha(v)beta(3) integrin receptor synergizes with radioimmunotherapy to increase efficacy and apoptosis in breast cancer xenografts. *Cancer Res* 62: 4263–4272, 2002
13) Carmeliet P, Jain RK: Angiogenesis in cancer and other diseases. *Nature* 407: 249–257, 2000
14) Chamberlain MC, Johnston SK: Salvage therapy with single agent bevacizumab for recurrent glioblastoma. *J Neurooncol* 96: 259–269, 2010

15) de Groot JF, Fuller G, Kumar AJ, Piao Y, Eterovic K, Ji Y, Conrad CA: Tumor invasion after treatment of glioblastoma with bevacizumab: radiographic and pathologic correlation in humans and mice. *Neuro-oncology* 12: 233–242, 2010
16) de Vries NA, Beijnen JH, van Tellingen O: High-grade glioma mouse models and their applicability for preclinical testing. *Cancer Treat Rev* 35: 714–723, 2009
17) Del Maestro RF, Megyesi JF, Farrell CL: Mechanisms of tumor-associated edema: a review. *Can J Neurol Sci* 17: 177–183, 1990
18) Eskens FA, Dumez H, Hoekstra R, Perschl A, Brindley C, Böttcher S, Wynendaele W, Drevs J, Verweij J, van Oosterom AT: Phase I and pharmacokinetic study of continuous twice weekly intravenous administration of Cilengitide (EMD 121974), a novel inhibitor of the integrins alphavbeta3 and alphavbeta5 in patients with advanced solid tumours. *Eur J Cancer* 39: 917–926, 2003
19) Esser S, Lampugnani MG, Corada M, Dejana E, Risau W: Vascular endothelial growth factor induces VE-cadherin tyrosine phosphorylation in endothelial cells. *J Cell Sci* 111 (Pt 13): 1853–1865, 1998
20) Ferrara N, Kerbel RS: Angiogenesis as a therapeutic target. *Nature* 438: 967–974, 2005
21) Forsyth PA, Wong H, Laing TD, Rewcastle NB, Morris DG, Muzik H, Leco KJ, Johnston RN, Brasher PM, Sutherland G, Edwards DR: Gelatinase-A (MMP-2), gelatinase-B (MMP-9) and membrane type matrix metalloproteinase-1 (MT1-MMP) are involved in different aspects of the pathophysiology of malignant gliomas. *Br J Cancer* 79: 1828–1835, 1999
22) Gilbert MR, Kuhn J, Lamborn KR, Lieberman F, Wen PY, Mehta M, Cloughesy T, Lassman AB, Deangelis LM, Chang S, Prados M: Cilengitide in patients with recurrent glioblastoma: the results of NABTC 03-02, a phase II trial with measures of treatment delivery. *J Neurooncol* 106: 147–153, 2012
23) Goodenough DA, Goliger JA, Paul DL: Connexins, connexons, and intercellular communication. *Annu Rev Biochem* 65: 475–502, 1996
24) Hanahan D, Folkman J: Patterns and emerging mechanisms of the angiogenic switch during tumorigenesis. *Cell* 86: 353–364, 1996
25) Henriksson R, Bottomley A, Mason W, et al: Progression-free survival (PFS) and health-related quality of life (HRQoL) in AVAglio, a phase III study of bevacizumab (Bv), temozolomide (T), and radiotherapy (RT) in newly diagnosed glioblastoma (GBM). 2013 ASCO Annual Meeting. Abstract 2005. Presented June 1, 2013
26) Holash J, Maisonpierre PC, Compton D, Boland P, Alexander CR, Zagzag D, Yancopoulos GD, Wiegand SJ: Vessel cooption, regression, and growth in tumors mediated by angiopoietins and VEGF. *Science* 284: 1994–1998, 1999
27) Inoue S, Ichikawa T, Kurozumi K, Maruo T, Onishi M, Yoshida K, Fujii K, Kambara H, Chiocca EA, Date I: Novel animal glioma models that separately exhibit two different invasive and angiogenic phenotypes of human glioblastomas. *World Neurosurg* 78: 670–682, 2012
28) Jain RK: Molecular regulation of vessel maturation. *Nat Med* 9: 685–693, 2003
29) Jain RK, di Tomaso E, Duda DG, Loeffler JS, Sorensen AG, Batchelor TT: Angiogenesis in brain tumours. *Nat Rev Neurosci* 8: 610–622, 2007
30) Jiang BH, Rue E, Wang GL, Roe R, Semenza GL: Dimerization, DNA binding, and transactivation properties of hypoxia-inducible factor 1. *J Biol Chem* 271: 17771–17778, 1996
31) Kevil CG, Payne DK, Mire E, Alexander JS: Vascular permeability factor/vascular endothelial cell growth factor-mediated permeability occurs through disorganization of endothelial junctional proteins. *J Biol Chem* 273: 15099–15103, 1998
32) Kim S, Bell K, Mousa SA, Varner JA: Regulation of angiogenesis in vivo by ligation of integrin alpha5beta1 with the central cell-binding domain of fibronectin. *Am J Pathol* 156: 1345–1362, 2000
33) Kireeva ML, Lam SC, Lau LF: Adhesion of human umbilical vein endothelial cells to the immediate-early gene product Cyr61 is mediated through integrin alphavbeta3. *J Biol Chem* 273: 3090–3096, 1998
34) Kurozumi K, Hardcastle J, Thakur R, Shroll J, Nowicki M, Otsuki A, Chiocca EA, Kaur B: Oncolytic HSV-1 infection of tumors induces angiogenesis and upregulates CYR61. *Mol Ther* 16: 1382–1391, 2008
35) Kurozumi K, Hardcastle J, Thakur R, Yang M, Christoforidis G, Fulci G, Hochberg FH, Weissleder R, Carson W, Chiocca EA, Kaur B: Effect of tumor microenvironment modulation on the efficacy of oncolytic virus therapy. *J Natl Cancer Inst* 99: 1768–1781, 2007
36) Lakka SS, Gondi CS, Rao JS: Proteases and glioma angiogenesis. *Brain Pathol* 15: 327–341, 2005
37) Lamszus K, Kunkel P, Westphal M: Invasion as limitation to anti-angiogenic glioma therapy. *Acta Neurochir Suppl* 88: 169–177, 2003
38) Leask A, Abraham DJ: All in the CCN family: essential matricellular signaling modulators emerge from the bunker. *J Cell Sci* 119: 4803–4810, 2006
39) Leavesley DI, Ferguson GD, Wayner EA, Cheresh DA: Requirement of the integrin beta 3 subunit for carcinoma cell spreading or migration on vitronectin and fibrinogen. *J Cell Biol* 117: 1101–1107, 1992
40) Lebelt A, Dziecioł J, Guzińska-Ustymowicz K, Lemancewicz D, Zimnoch L, Czykier E: Angiogenesis in gliomas. *Folia Histochem Cytobiol* 46: 69–72, 2008
41) Lindahl P, Johansson BR, Levéen P, Betsholtz C: Pericyte loss and microaneurysm formation in PDGF-B-deficient mice. *Science* 277: 242–245, 1997
42) Lopes MB: Angiogenesis in brain tumors. *Microsc Res Tech* 60: 225–230, 2003
43) MacDonald TJ, Taga T, Shimada H, Tabrizi P, Zlokovic BV, Cheresh DA, Laug WE: Preferential susceptibility of brain tumors to the antiangiogenic effects of an alpha(v) integrin antagonist. *Neurosurgery* 48: 151–157, 2001
44) Maisonpierre PC, Suri C, Jones PF, Bartunkova S,

Wiegand SJ, Radziejewski C, Compton D, McClain J, Aldrich TH, Papadopoulos N, Daly TJ, Davis S, Sato TN, Yancopoulos GD: Angiopoietin-2, a natural antagonist for Tie2 that disrupts in vivo angiogenesis. *Science* 277: 55–60, 1997

45) Mandriota SJ, Seghezzi G, Vassalli JD, Ferrara N, Wasi S, Mazzieri R, Mignatti P, Pepper MS: Vascular endothelial growth factor increases urokinase receptor expression in vascular endothelial cells. *J Biol Chem* 270: 9709–9716, 1995
46) Maruo T, Ichikawa T, Kanzaki H, Inoue S, Kurozumi K, Onishi M, Yoshida K, Kambara H, Ouchida M, Shimizu K, Tamaru S, Chiocca EA, Date I: Proteomics-based analysis of invasion-related proteins in malignant gliomas. *Neuropathology* 33: 264–275, 2013
47) Mikkelsen T, Brodie C, Finniss S, Berens ME, Rennert JL, Nelson K, Lemke N, Brown SL, Hahn D, Neuteboom B, Goodman SL: Radiation sensitization of glioblastoma by cilengitide has unanticipated schedule-dependency. *Int J Cancer* 124: 2719–2727, 2009
48) Nagano O, Saya H: Mechanism and biological significance of CD44 cleavage. *Cancer Sci* 95: 930–935, 2004
49) Onishi M, Ichikawa T, Kurozumi K, Date I: Angiogenesis and invasion in glioma. *Brain Tumor Pathol* 28: 13–24, 2011
50) Onishi M, Ichikawa T, Kurozumi K, Fujii K, Yoshida K, Inoue S, Michiue H, Chiocca EA, Kaur B, Date I: Bimodal anti-glioma mechanisms of cilengitide demonstrated by novel invasive glioma models. *Neuropathology* 33: 162–174, 2013
51) Onishi M, Kurozumi K, Ichikawa T, Michiue H, Fujii K, Ishida J, Shimazu Y, Chiocca EA, Kaur B, Date I: Gene expression profiling of the anti-glioma effect of Cilengitide. *Springerplus* 2: 160, 2013
52) Rao JS, Yamamoto M, Mohaman S, Gokaslan ZL, Fuller GN, Stetler-Stevenson WG, Rao VH, Liotta LA, Nicolson GL, Sawaya RE: Expression and localization of 92 kDa type IV collagenase/gelatinase B (MMP-9) in human gliomas. *Clin Exp Metastasis* 14: 12–18, 1996
53) Reardon DA, Fink KL, Mikkelsen T, Cloughesy TF, O'Neill A, Plotkin S, Glantz M, Ravin P, Raizer JJ, Rich KM, Schiff D, Shapiro WR, Burdette-Radoux S, Dropcho EJ, Wittemer SM, Nippgen J, Picard M, Nabors LB: Randomized phase II study of cilengitide, an integrin-targeting arginine-glycine-aspartic acid peptide, in recurrent glioblastoma multiforme. *J Clin Oncol* 26: 5610–5617, 2008
54) Reifenberger G, Collins VP: Pathology and molecular genetics of astrocytic gliomas. *J Mol Med* 82: 656–670, 2004
55) Reiss Y, Machein MR, Plate KH: The role of angiopoietins during angiogenesis in gliomas. *Brain Pathol* 15: 311–317, 2005
56) Rooprai HK, McCormick D: Proteases and their inhibitors in human brain tumours: a review. *Anticancer Res* 17: 4151–4162, 1997
57) Salhia B, Rutten F, Nakada M, Beaudry C, Berens M, Kwan A, Rutka JT: Inhibition of Rho-kinase affects astrocytoma morphology, motility, and invasion through activation of Rac1. *Cancer Res* 65: 8792–8800, 2005
58) Sathornsumetee S, Reardon DA, Desjardins A, Quinn JA, Vredenburgh JJ, Rich JN: Molecularly targeted therapy for malignant glioma. *Cancer* 110: 13–24, 2007
59) Stupp R, Van Den Bent MJ, Erridge SC, Reardon DA, Hong Y, Wheeler H, Hegi M, Perry JR, Picard M, Weller M: Cilengitide in newly diagnosed glioblastoma with MGMT promoter methylation: protocol of a multicenter, randomized, open-label, controlled phase III trial (CENTRIC). *J Clin Oncol* 28: 15s, 2010
60) Tate MC, Aghi MK: Biology of angiogenesis and invasion in glioma. *Neurotherapeutics* 6: 447–457, 2009
61) Tentori L, Dorio AS, Muzi A, Lacal PM, Ruffini F, Navarra P, Graziani G: The integrin antagonist cilengitide increases the antitumor activity of temozolomide against malignant melanoma. *Oncol Rep* 19: 1039–1043, 2008
62) Wenger RH, Stiehl DP, Camenisch G: Integration of oxygen signaling at the consensus HRE. *Sci STKE* 2005: re12, 2005
63) Wesseling P, Ruiter DJ, Burger PC: Angiogenesis in brain tumors; pathobiological and clinical aspects. *J Neurooncol* 32: 253–265, 1997
64) Wild-Bode C, Weller M, Wick W: Molecular determinants of glioma cell migration and invasion. *J Neurosurg* 94: 978–984, 2001
65) Wong ML, Prawira A, Kaye AH, Hovens CM: Tumour angiogenesis: its mechanism and therapeutic implications in malignant gliomas. *J Clin Neurosci* 16: 1119–1130, 2009
66) Zagzag D, Amirnovin R, Greco MA, Yee H, Holash J, Wiegand SJ, Zabski S, Yancopoulos GD, Grumet M: Vascular apoptosis and involution in gliomas precede neovascularization: a novel concept for glioma growth and angiogenesis. *Lab Invest* 80: 837–849, 2000
67) Zagzag D, Goldenberg M, Brem S: Angiogenesis and blood-brain barrier breakdown modulate CT contrast enhancement: an experimental study in a rabbit brain-tumor model. *AJR Am J Roentgenol* 153: 141–146, 1989
68) Zagzag D, Hooper A, Friedlander DR, Chan W, Holash J, Wiegand SJ, Yancopoulos GD, Grumet M: In situ expression of angiopoietins in astrocytomas identifies angiopoietin-2 as an early marker of tumor angiogenesis. *Exp Neurol* 159: 391–400, 1999

Address reprint requests to: Manabu Onishi, MD, PhD, Department of Neurological Surgery, Okayama University Graduate School of Medicine, Dentistry and Pharmaceutical Sciences, 2-5-1 Shikata-cho, Okayama, Okayama 700-8558, Japan.
e-mail: onishi_manabu@yahoo.co.jp

NEUROPATHOLOGY

Neuropathology 2013; **33**, 264–275 doi:10.1111/j.1440-1789.2012.01361.x

Original Article

Proteomics-based analysis of invasion-related proteins in malignant gliomas

Tomoko Maruo,[1] Tomotsugu Ichikawa,[1] Hirotaka Kanzaki,[2] Satoshi Inoue,[1] Kazuhiko Kurozumi,[1] Manabu Onishi,[1] Koichi Yoshida,[1] Hirokazu Kambara,[1] Mamoru Ouchida,[2] Kenji Shimizu,[2] Seiji Tamaru,[3] E. Antonio Chiocca[4] and Isao Date[1]

[1]Department of Neurological Surgery, [2]Department of Molecular Genetics, Okayama University Graduate School of Medicine, Dentistry and Pharmaceutical Sciences, [3]Central Research Laboratory, Okayama University Medical School, Okayama, Japan, and [4]Department of Neurosurgery, Brigham and Women's/ Faulkner Hospital, Boston, Massachusetts, USA

One of the insidious biological features of gliomas is their potential to extensively invade normal brain tissue, yet molecular mechanisms that dictate this locally invasive behavior remain poorly understood. To investigate the molecular basis of invasion by malignant gliomas, proteomic analysis was performed using a pair of canine glioma subclones – J3T-1 and J3T-2 – that show different invasion phenotypes in rat brains but have similar genetic backgrounds. Two-dimensional protein electrophoresis of whole-cell lysates of J3T-1 (angiogenesis-dependent invasion phenotype) and J3T-2 (angiogenesis-independent invasion phenotype) was performed. Twenty-two distinct spots were recognized when significant alteration was defined as more than 1.5-fold change in spot intensity between J3T-1 and J3T-2. Four proteins that demonstrated increased expression in J3T-1, and 14 proteins that demonstrated increased expression in J3T-2 were identified using liquid chromatography-mass spectrometry analysis. One of the proteins identified was annexin A2, which was expressed at higher levels in J3T-1 than in J3T-2. The higher expression of annexin A2 in J3T-1 was corroborated by quantitative RT-PCR of the cultured cells and immunohistochemical staining of the rat brain tumors. Moreover, immunohistochemical analysis of human glioblastoma specimens showed that annexin A2 was expressed at high levels in the tumor cells that formed clusters around dilated vessels. These results reveal differences in the proteomic profiles between these two cell lines that might correlate with their different invasion profiles. Thus, annexin A2 may be related to angiogenesis-dependent invasion.

Key words: angiogenesis, annexin A2, glioma, invasion, proteomics.

INTRODUCTION

Gliomas are highly invasive and tend to diffusely infiltrate the brain, thereby placing tumor cells outside the margins of therapeutic resection. The mechanisms of invasion by glioma cells have been addressed in different studies and experimental settings, yet there is a need for a novel panel of biomarkers that characterize each invasive phenotype. Moreover, invasive nests of tumor cells are associated with initiation of neovascular angiogenesis and disruption of the blood–brain barrier through release of vasomodulatory cytokines. Taken together, these factors contribute to the rapid invasion process that is beyond the confines of the typical radiologically identifiable tumor mass, resulting in the near universally high rate of tumor recurrence and ultimate death.

Little is known about the distinct biology of invasive gliomas *in situ,* but their diffuse invasion profile suggests the activation of genetic and cellular mechanisms that distinguish them from the cells inside the tumor's core. Systematic analysis of tumor cells with different biological behaviors may help to elucidate the nature of each tumor's invasion pattern. Currently, the proteomic approach has made it possible to characterize the global alterations that occur in cellular protein expression. This proteomics-based analysis promises new insights into the cellular mechanisms involved in tumor invasion and is likely to result in the discovery of novel diagnostic markers and new therapeutic targets.

Correspondence: Tomotsugu Ichikawa, MD, PhD, Department of Neurological Surgery, Okayama University Graduate School of Medicine, Dentistry and Pharmaceutical Sciences, Address: 2-5-1, Shikata-cho, Kita-ku, Okayama 700-8558, Japan. Email: tomoichi@cc.okayama-u.ac.jp

Received 11 August 2012; revised 27 September 2012 and accepted 3 October 2012; published online 1 November 2012.

In our previous study, detailed histopathological observations of human glioblastoma tissue revealed that there are at least two invasive and angiogenic phenotypes: one dependent on angiogenesis and the other independent of angiogenesis. Glioma cells migrate along dilated vessels in angiogenesis-dependent invasion, while infiltration of single glioma cells into the brain tissue is unrelated to the vasculature in angiogenesis-independent invasion.[1,2] Moreover, we established two glioma cell lines (J3T-1 and J3T-2) that showed different invasion phenotypes when implanted in rat brains.[1,2] J3T-1 cells form comparatively well-demarcated and highly angiogenic tumors, while J3T-2 cells form tumors with obscure margins via single-cell infiltration into the normal brain parenchyma. J3T-1 and J3T-2 cells show angiogenesis-dependent and independent invasive patterns, respectively, in rat brain tumor models; these patterns resemble those of human glioblastoma invasion.

In the present study, this pair of cell lines was examined using a proteomics approach, including the use of two-dimensional gel electrophoresis (2DGE) and liquid chromatography-tandem mass spectrometry analysis (LC-MS/MS), to compare the proteomic profiles of these two cell lines with different invasion phenotypes.

MATERIALS AND METHODS

Cell culture

The J3T canine glioma cell was a generous gift from Michael E. Berens, MD, PhD (Translation Genomics Research Institute, Phoenix, AZ, USA).[3] Two cell lines – J3T-1 and J3T-2 – were developed from the parental J3T cell line, as previously described.[1,4] In brief, J3T cells (5×10^6 cells) were subcutaneously implanted into the flanks of two athymic mice (NCr/Sed, nu/nu, 20 g). After 6 weeks, two tumors were established in each animal. These tumors were harvested in a sterile fashion, minced with a scalpel into 1 mm^3 cubes, treated for 1 h with 1 mg/mL collagenase/dispase (Roche, Basel, Switzerland), and subsequently cultured in DMEM supplemented with 10% fetal bovine serum (FBS), 100 units penicillin, and 0.1 mg/mL streptomycin. Both cell lines were derived from single subcutaneous tumors.

For enhanced visualization of J3T-1 and J3T-2 cells, cell lines were established which stably expressed green fluorescent protein (GFP), as previously described.[1] In brief, J3T-1 and J3T-2 cells were transfected with the pAcGFP1-C1 plasmid (Clontech Laboratories Inc, Mountain View, CA, USA), which encodes for GFP using the TransIT-LT1 reagent (Takara Bio Inc, Otsu, Japan) to obtain J3T-1G and J3T-2G, respectively. Cells were cultured in DMEM supplemented with 10% FBS, 100 units penicillin, and 0.1 mg/mL streptomycin in a standard tissue incubator at 37°C with a 5% CO_2 atmosphere.

2DGE

The cells were washed with a PBS solution that contained 0.27% $CaCl_2 \cdot H_2O$, 0.02% $MgCl_2 \cdot 6H_2O$, 1% FBS, and 5 mmol/L sodium pyruvate. Cells were harvested by mechanical scraping during the exponential growth phase. Cells were then centrifuged, and the cell pellets were dissolved in a lysis buffer that consisted of 5 mol/L urea, 2 mol/L thiourea, 2% 3-(3-cholamidopropyl)dimethylammonio-1-propane sulfonate (CHAPS), 2% sulfobetaine 3–10 (SB3-10), 1% dithiothreitol (DTT), and a protease inhibitor cocktail (Sigma-Aldrich, St. Louis, MO, USA). After three freeze–thaw cycles, the cell pellets were sonicated for 30 s and ultracentrifuged at $75\,000 \times g$ for 30 min at 10°C using the Optima™ TLX ultracentrifuge (Beckman Coulter, Brea, CA, USA). The supernatant was transferred to a new tube and treated with ReadyPrep 2D Cleanup Kit (Bio-Rad, Hercules, CA, USA) to remove any ions, DNA, RNA and so on. The protein concentration was estimated using the RC-DC Protein Assay kit (Bio-Rad) according to the manufacturer with a two-washed standard protocol. For isoelectric focusing (IEF), Carrier ampholyte 5/8 (Bio-Rad) was formulated to increase the resolution at the basic end of the flatbed isoelectric focusing gel.

The first-dimensional IEF was performed using a 17-cm immobilized nonlinear pH gradient (5–8) strip (DryStrip; Bio-Rad). After rehydration for 15 h in a 300-µL buffer that consisted of 5 mol/L urea, 2 mol/L thiourea, 2% CHAPS, 3% SB3-10, 1% DTT, and 0.2% Bio-Lyte® 5/8 ampholyte (Bio-Rad), 60-µg samples of each protein were loaded onto the strips. Focusing was performed in the following steps: (i) 250 V with linear increase for 40 min; (ii) 10 000 V with linear increase for 4 h; and (iii) 10 000 V with rapid increase for 7 h (total 70 000 V-h). The samples were then maintained at 500 V, as needed.

The focused strips were then equilibrated in buffer I (6 mol/L urea, 2% SDS, 0.375 mol/L Tris-HCl, 20% glycerol, and 2% DTT; pH 8.8) for 30 min and then buffer II (6 mol/L urea, 2% SDS, 0.375 mol/L Tris-HCl, 20% glycerol, and 2.5% iodoacetamide; pH 8.8) for 15 min with gentle shaking. The second-dimensional separation was carried out on 12% SDS-polyacrylamide gels using PROTEAN II Cell (Bio-Rad) at 20°C and 40 mA/gel for 4 h.

After 2DGE, the gels were stained with SYPRO Ruby (Invitrogen, Carlsbad, CA, USA) and Dodeca Silver Stain Kits (Bio-Rad), according to the manufacturer's protocols. Each experiment was performed in triplicate.

Image analysis of 2DGE gels

Images of the SYPRO Ruby-stained gels were obtained using a FLA-3000 image analyzer (Fujifilm, Tokyo, Japan). The images were analyzed using PDQuest Advanced, version 8.0 (Bio-Rad); analysis included background subtraction, spot detection, and volume normalization. The intensity of each spot was quantified by calculating the spot volume after normalization to the local regression model. The intensities of three sets of matched spots of each J3T-1 and J3T-2 gel were compared, and a threshold ratio of 1.5 was used to screen for differences. Visual inspection confirmed the differences indicated by PDQuest analysis.

Protein identification

The selected protein spots were manually excised from the gels after visualizing the spots with silver staining. After destaining and drying the excised spots, in-gel trypsin digestion using the Protein In-Gel Tryptic Digestion kit (Agilent Technologies, Santa Clara, CA, USA) was performed overnight at 30°C. The obtained peptide digests were analyzed using a fully automated nanoflow liquid chromatography-ion trap-tandem mass spectrometer (nLC-IT-MS/MS; Agilent 1100 LC/MSD Trap XCT Ultra, Agilent Technologies).

Protein identification was performed using the Spectrum Mill MS Proteomics Workbench platform (version A.03.02; Agilent Technologies), according to the workflow parameters specified by the manufacturer. The identification parameters were set as follows: database, NCBInr; species, Canis familialis; enzyme, trypsin; monoisotopic masses used; precursor mass tolerance (peptide tolerance), ±2.5 Da; product mass tolerance (MS/MS tolerance), ±0.8; fixed modification, carbamidomethylation (cysteine); and variable modification, oxidation (methionine). Two missed cleavages with trypsin were allowed and the instrument's setting was specified as "ESI ion trap". The probability scores calculated by the software were used as the criteria for correct identification.

Quantitative RT-PCR)

Total RNA was isolated from cultured J3T-1 and J3T-2 cells using RNeasy® Mini Kit (QIAGEN, Valencia, CA, USA) and reverse-transcribed with oligo dT primers using SuperScript III First-Strand Synthesis System for RT-PCR (Invitrogen), according to the manufacturer's instructions. Primers specific for each target gene were designed using Primer Express (Applied Biosystems, Foster City, CA, USA) and synthesized by Invitrogen. The resulting cDNA was amplified by PCR using gene-specific primers and the 7300 Real Time PCR system (Applied Biosystems) and QuantiTect™ SYBR® Green PCR kit (QIAGEN). A log-linear relationship between the amplification curve and quantity of cDNA in the range of 1 to 1000 copies was observed.

The cycle number at the threshold was used as the threshold cycle (Ct). The different expression of mRNA was deducted from $2^{-\Delta\Delta Ct}$ using the 7300 Real Time PCR System with the Sequence Detection software (version 1.4; Applied Biosystems). The amount of cDNA in each sample was normalized to the crossing point of the housekeeping gene *GAPDH*. The following thermal cycling parameters were used: denaturation at 95°C for 15 min, followed by 40 cycles of 30 s at 94°C, 30 s at 55°C, and 1 min at 72°C. The relative mRNA upregulation for each gene in the J3T-2 cells was calculated using their respective crossing points in the following formula:

$$F = 2^{(TH-TG)-(OH-OG)}$$

where, F = fold difference, T = J3T – 2 cells, O = J3T – 1 cells, H = housekeeping gene (*GAPGH*) and G = gene of interest.

Immunohistochemistry

All experimental animals were housed and handled in accordance with the Okayama University Animal Research Committee guidelines. Before implantation, 85–90% of the confluent J3T-1, J3T-2, J3T-1G and J3T-2G cells were trypsinized, rinsed with a solution of DMEM and 10% FBS, and centrifuged at 116 × *g* for 5 min. The resulting pellets were resuspended in PBS and the concentration was adjusted to 1×10^5 cells/μL of PBS. To establish the brain tumor models, athymic rats (F344/N-nu/nu; CLEA Japan, Inc., Tokyo, Japan) were anesthetized with an intraperitoneal injection of nembutal (30 mg/kg) and placed in a stereotactic apparatus (Narishige, Tokyo, Japan). Tumor cells (5×10^5 cells/5 μL) were slowly injected into the basal ganglia of the right cerebral hemisphere (4 mm lateral and 1 mm anterior to the bregma at a depth of 4 mm) using a Hamilton syringe (Hamilton, Reno, NV, USA), according to previously published procedures.[1,5] For histological examination, the athymic rats (J3T-1, $n = 5$; J3T-2, $n = 5$) were sacrificed 4–5 weeks after tumor inoculation. Before sacrificing, the animals were anesthetized. Death was induced via cardiac puncture, then the animals were perfused with 100 mL PBS and fixated with 200 mL of 4% paraformaldehyde. The brains were removed and stored in 4% paraformaldehyde for at least 24 h. Snap-frozen tissue samples were embedded in an optimal cutting temperature compound for cryosectioning. Sixteen-micrometer cryostat sections were processed for indirect immunofluorescence analysis. The slides were incubated with 10% horse serum in PBS at room temperature and then with the anti-annexin A2 antibody (1:20 mouse IgG;

Zymed Laboratories, San Francisco, CA, USA) diluted with 1% horse serum in PBS, and stored overnight at 4°C. After three washes with PBS for 5 min, the slides were incubated with Cy3-conjugated antibodies against mouse IgG (1:300) (Jackson ImmunoResearch Laboratories, Inc., West Grove, PA, USA) and 4′,6-diamino-2-phenylindole in PBS (1:500; Invitrogen) for 60 min. The slides were then washed with PBS and mounted.

Human glioma samples were intraoperatively obtained from patients undergoing surgical removal of tumors for diagnostic and therapeutic purposes (Okayama University Hospital, Okayama, Japan). Written informed consent was taken in all the cases before surgery. Lobectomies were performed to remove the entire tumor and any surrounding brain parenchyma beyond the boundaries of the tumors observed on MRI. All glioma specimens were diagnosed and graded according to the World Health Organization classification of tumors of the CNS, and all five specimens were diagnosed as glioblastomas. No patient had received radiation or chemotherapy before surgery.

After deparaffinization in xylene and rehydration in decreasing concentrations of ethanol, 4-μm-thick sections were incubated in 0.3% hydrogen peroxide (30 min) and autoclaved with distilled water for 10 min at 121°C. After three washes in PBS, the sections were incubated with anti-annexin A2 monoclonal antibodies (1:20) (mouse IgG; Zymed Laboratories) that had been diluted with PBS and 5% skim milk (60 min) at room temperature. A secondary antibody was applied using the DakoCytomation Envision+ System-HRP kit, according to the manufacturer's protocol (DakoCytomation, Carpinteria, CA, USA). The sections were visualized using 3,3′-diaminobenzidine (DAB).

Annexin A2 expression was qualitatively scored as follows: (–) for no staining (nearly 0% of cells were labeled), (+) for a trace of positive cells (less than 30% of cells were labeled), (++) for moderately diffuse staining or sparsely intensive staining (30%–60% of cells were labeled, and less than 30% of cells were labeled with the strong intensity), and (+++) for strongly diffuse staining (60%–100% of cells were labeled). TM and SI classified the tumors according to three representative fields without prior knowledge of the patients' clinical or radiological data.

RESULTS

2DGE patterns and differential analysis of J3T-1 and J3T-2

The 2DGE gel images of J3T-1 and J3T-2 cells showed similar protein expression patterns, probably reflecting the genetic similarity of J3T-1 and J3T-2 (Fig. 1).

Using the PDQuest 2DGE gel analysis software, approximately 2800 well-stained and clearly delineated protein spots were detected. Twenty-two spots showed more than 1.5-fold change in spot intensity; five of these protein spots were upregulated in J3T-1 and 17 were upregulated in J3T-2. These differentially expressed protein spots are illustrated with circles and spot numbers in Figure 1a,b.

Proteins identified by LC-MS/MS

Differentially expressed protein spots were excised from the 2DGE gels and analyzed for protein identification by LC-MS/MS and database searching. As a result, 18 proteins were identified in those spots; these proteins are shown in Table 1. The Spectrum Mill software calculates the MS/MS search score as described below. Each peak assigned to an allowed fragment ion type for a candidate peptide sequence is given "bonus points". In contrast, each unassigned peak is given "penalty points". Penalty

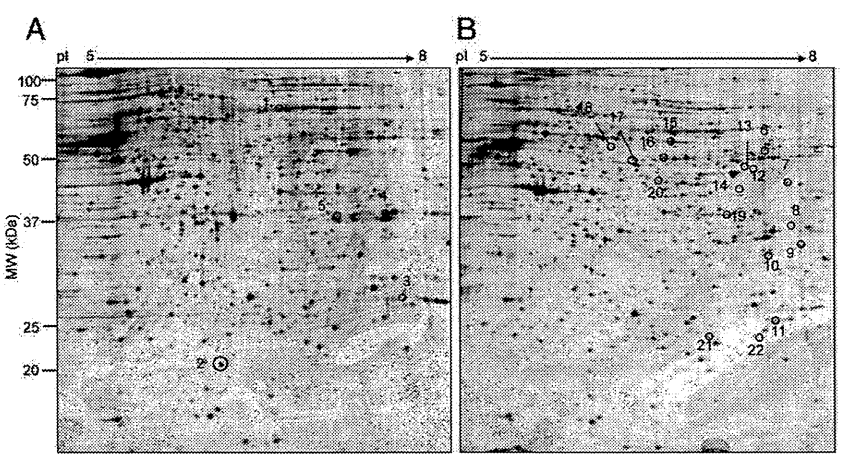

Fig. 1 SYPRO Ruby-stained two-dimensional gel electrophoresis (2DGE) gel images of J3T-1 (a) and J3T-2 (b) cells. The arabic numbers indicate the differentially expressed spots; the numbers refer to those reported in Table 1. The protein expression levels of spots 1–5 were upregulated in J3T-1 cells. The protein expression levels of spots 6–22 were upregulated in J3T-2 cells. pI, isoelectric point; MW, molecular weight; Da, Daltons.

Table 1 Results of differentially expressed proteins in J3T-1 and J3T-2 cells

Spot no.†	Protein name	NCBI-AC‡	MW(Da)/pI	AA§(%)	MS/MS score	Potential biological function
Up-regulated in J3T-1						
1	Prelamin A/C isoform 4	XP_864434	74226/6.57	40	408.01	Structural protein components of the nuclear lamina
2	Ferritin light chain 2	XP_536874	28397.3/5.39	14	55.69	Storage protein (iron ion transport)
3	Triosephosphate isomerase	NP_001183983	26714.7/6.9	28	82.69	Metabolic enzyme (fatty acid biosynthesis, gluconeogenesis, glycolysis)
4	Annexin A2	NP_001002961	38654.3/6.92	6	26	Calcium-dependent phospholipid-binding protein, regulation of cellular growth and in signal transduction pathways
5	Not identified					
Up-regulated in J3T-2						
6	3-oxoacid CoA transferase 1	XP_536487	64746/7.91	12	103.21	Metabolic enzyme (ketone body catabolism)
7	Glycine amidinotransferase, mitochondrial	XP_544663	48379.7/8.59	21	119.73	Metabolic enzyme (creatine biosynthesis)
8	Aminoacyl tRNA synthase complex-interacting multifunctional protein 2-like (AIMP2)	XP_536880	35298.8/7.07	12	37.41	Translation regulatory protein, protein metabolism
9	Heterogeneous nuclear ribonucleoprotein A1 (HNRNPA1)	XP_851182	42254.5/9.27	6	29	RNA-binding protein (regulation of nucleobase, nucleoside, nucleotide and nucleic acid metabolism)
10	Sulfotransferase 1C4	XP_531771	35461.8/6.87	10	40.15	Metabolic enzyme (energy pathway)
11	Glutathione S-transferase theta 1-like isoform4	XP_857014	27639.3/6.66	15	35.11	Metabolic enzyme (energy pathway)
12	Elongation factor 2	XP_533949	77884/6.34	5	47.47	Translation regulatory protein, protein metabolism
13	Septin 11	XP_535616	52111.6/6.24	8	45.17	GTP-binding protein (GTPase activity, cell cycle, vesicle-mediated transport)
14	Fatty acid synthase	XP_540497	268846.4/5.99	2	87.67	Metabolic enzyme (energy pathway, catalytic activity)
15	Dihydropyrimidinase-related protein 3	XP_544332	94582/7.08	24	275.93	Metabolic enzyme (energy pathway, hydrolase activity)
16	D-3-phosphoglycerate dehydrogenase-like	XP_849835	56545.8/6.19	17	141.56	Metabolic enzyme (Energy pathway, catalytic activity)
17	Aldehyde dehydrogenase mitochondrial isoform 2 (ALDH2),	XP_853628	56763.1/6.63	25	176.99	Metabolic enzyme (Energy pathway, catalytic activity)
18	Heterogeneous nuclear ribonucleoprotein K isoform a isoform 1 (HNRNPK)	XP_533511	50890.4/5.31	18	116.18	RNA-binding protein
19	Mitogen-activated protein kinase 1	XP_860750	42880.5/6.28	16	88.01	Signal transduction, cell communication (serine/threonine kinase activity)
20	Not identified					
21	Not identified					
22	Not identified					

†Protein spot numbers corresponded to the two-dimensional gel electrophoresis image in Figure 1. ‡Accession code in NCBI. §Amino acid coverage (%). Da, Daltons; MW, theoretical molecular weight; pI, theoretical isoelectric point.

value is based on peak height, – (peak height/height of tallest peak). MS/MS score is the summation of these bonus points and penalty points, indicating probability of the protein. Thus, the higher score indicates the better probability. The identified proteins that were upregulated in J3T-1 included one metabolic enzyme, one storage protein, one structural protein, and one phospholipid-binding protein. Proteins that were upregulated in J3T-2 included eight metabolic enzymes, two translational regulatory proteins, two RNA-binding proteins, one guanosine triphosphate (GTP)-binding protein, and one signal transduction protein. Metabolic enzymes constituted more than half of the proteins that were upregulated in J3T-2.

Figure 2a,b shows the distribution of all 18 identified proteins that were upregulated in J3T-1 and J3T-2 according to their general functions as described in NCBI Entrez Gene Database (http://www.ncbi.nlm.nih.gov/sites/entrez?db=gene) and Human Protein Reference Database (http://www.hprd.org/index_html). Figure 2c shows the representative MS/MS spectrum for the peptide sequence matched to annexin A2 identified from spot No.4.

Candidate protein validation by quantitative RT-PCR

A summary of the quantitative RT-PCR data is shown in Figure 3. Similar patterns were observed for the gene expression profiles obtained with the proteomics and quantitative RT-PCR data. The directionality of expression of 17 of the 18 genes coincided with the expression of the corresponding proteins. Fourteen of 18 genes demonstrated more than 1.5-fold change in expression (as denoted by the asterisks in Fig. 3), while the rest of the proteins did not show marked difference in expression between J3T-1 and J3T-2 cells.

Immunohistochemical corroboration of candidate proteins observed in the invasive animal models

Representative photomicrographs of the invasive animal models are presented in Figure 4a,b. J3T-1 cells formed well-demarcated and highly angiogenic tumors. In contrast, J3T-2 cells formed tumors with obscure margins via single-cell infiltration into the normal brain parenchyma.

The results of this proteomics-based analysis of the proteins involved in invasion were corroborated by

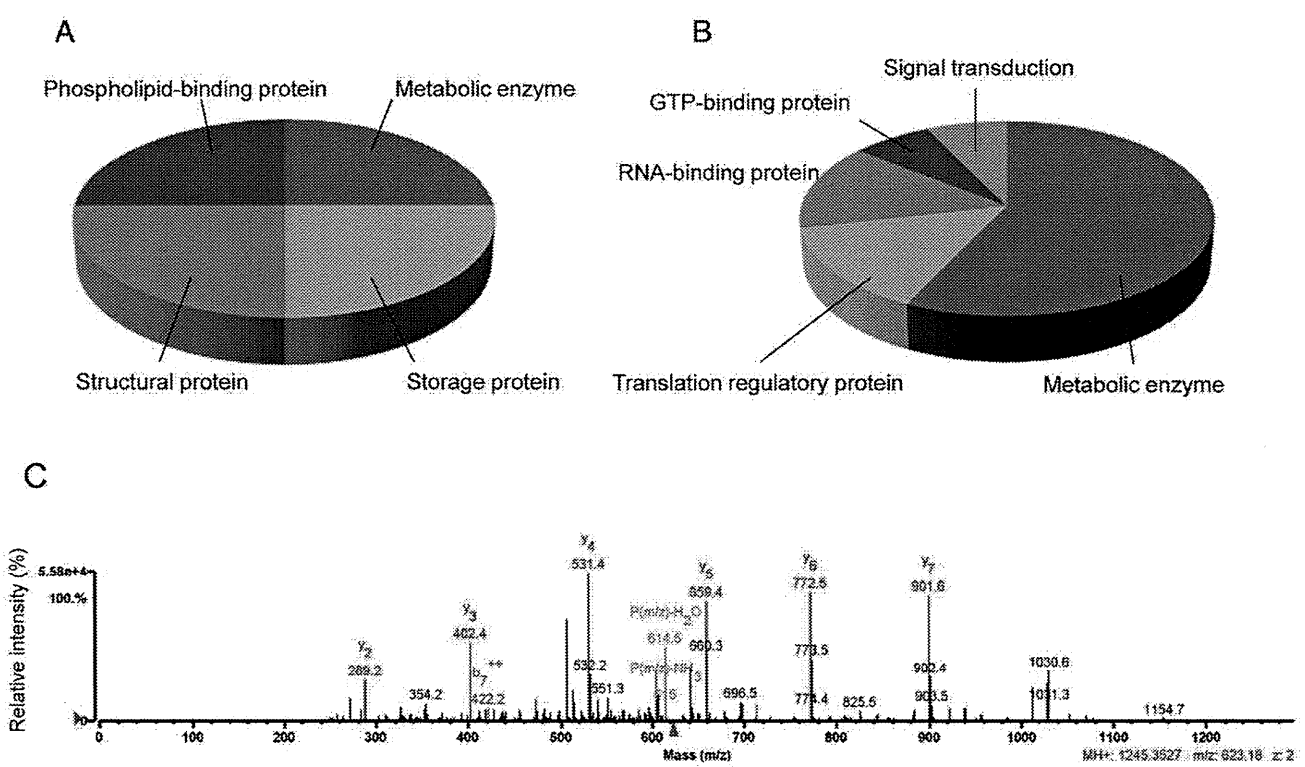

Fig. 2 Distribution of proteins according to their function and representative tandem mass (MS/MS) spectrum. (a and b) Pie charts representing the distribution of the identified proteins according to their general functions. Assignments were made on the basis of information provided from the NCBI Entrez Gene and Human Protein Reference Database. (a) Upregulated proteins in J3T-1 cells. (b) Upregulated proteins in J3T-2 cells. (c) The representative MS/MS spectrum for the peptide sequence matched to annexin A2.

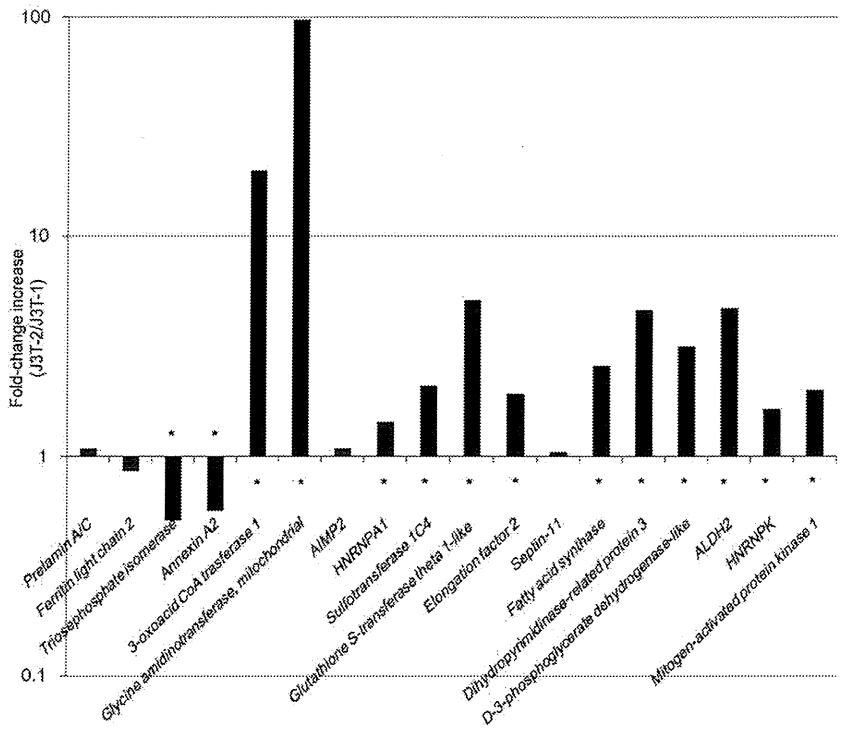

Fig. 3 Quantitative RT-PCR validation of candidate proteins shown to be differentially expressed in J3T-1 and J3T-2 cells by proteomic analysis. The names of the analyzed transcripts are listed along the *x*-axis and the fold-change increases of each gene in J3T-1 versus J3T-2 cells (i.e., differences in the relative copy numbers, where 1 represents equal expression levels in both populations) are listed along the *y*-axis. Asterisks denote genes that demonstrated more than 1.5-fold change in expression levels.

immunohistochemical analysis of the J3T-1G and J3T-2G xenograft models. One of the identified proteins was annexin A2, which has been reported to be involved in tumor invasion and metastasis.[6–8] Therefore, this protein was further studied using both animal models and human glioma samples. The annexin A2 antibody was readily available for immunohistochemical analysis of the frozen sections. Intense staining of the annexin A2 protein in the cytoplasm of the J3T-1 tumor cells was observed, whereas almost no staining was observed in the J3T-2 tumor cells (Fig. 4c–h), as expected based on the results of the proteomic analysis.

Immunohistochemical analysis of annexin A2 in human glioma samples

To analyze expression pattern of annexin A2 in relation to vasculature, immunohistochemical staining with anti-annexin A2 antibody was performed in five human glioblastoma samples. Patient age, sex, tumor locations, and degree of annexin A2 expression are summarized in Table 2. The center of the tumor comprised an area of high-density tumor cells which were negative or weakly positive for annexin A2. Marked angiogenesis, which was characterized by thick endothelial proliferation, was seen in the center and at the tumor borders. At the borders, clusters of annexin A2-positive tumor cells were observed around dilated vessels in all cases (Fig. 5a). Furthermore, diffuse single cell infiltration from the tumor core to the surrounding normal brain parenchyma, which was independent of vascular structure, was observed. Those cells were mostly negative (four cases) or weakly positive (one case; Patient 3) for annexin A2 (Fig. 5b).

DISCUSSION

To investigate the molecular basis of the invasive properties of malignant gliomas, proteomic analysis of the invasion-related proteins was performed using two unique sibling glioma cell lines, J3T-1 and J3T-2, which exhibit different aspects of human glioma invasion *in situ*.

Advantages of the proteomic method for identifying invasion-related proteins

This study describes how four proteins were observed in J3T-1 cells and 14 proteins were observed in J3T-2 cells, out of 2800 protein spots that were reproducibly identified on 2DGE gels at pH 5–8.

The similarities in the protein expression patterns on the 2DGE gel images of J3T-1 and J3T-2 cells reflect their genetic proximity. At the same time, significant differences in protein expression between these two cell lines do exist, which could be directly related to their invasive characteristics. Taken together, the proteomic method could be used to sensitively capture the features of the cell lines used in this study.

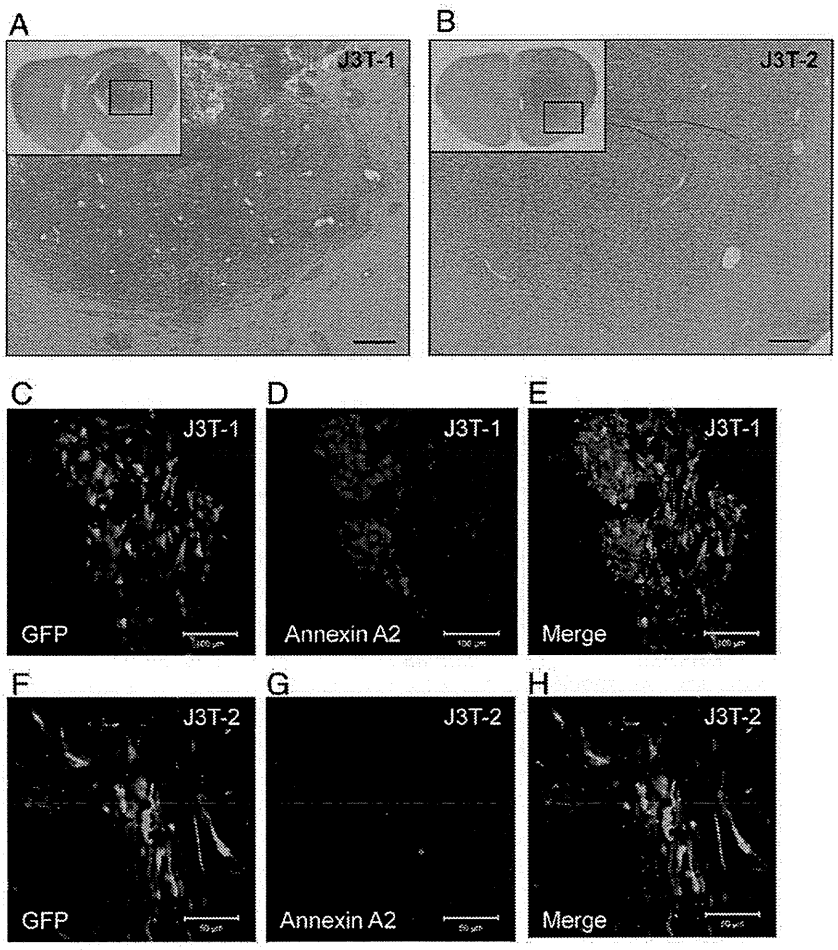

Fig. 4 *In vivo* analysis of the invasive animal model. Macroscopic and microscopic appearance of two distinct invasion phenotypes in athymic rats harboring J3T-1 (a) and J3T-2 (b) brain tumors are shown. J3T-1 cells form well-demarcated and highly angiogenic tumors. Multiple small satellite tumors are also observed at the tumor borders. J3T-2 cells gradually dispersed from the tumor center to the surrounding normal brain tissue. All sections are stained with HE. Bars indicate 300 μm. Immunohistochemical analysis of annexin A2 was performed using rat brain samples that harbored green fluorescent protein (GFP)-expressing J3T-1 (c, d, e) and J3T-2 (f, g, h) brain tumors. The annexin A2 antibody was visualized using the Cy3-conjugated secondary antibody (red). The remarkable staining of annexin A2 in the cytoplasm of J3T-1 tumor cells is shown (d, e); J3T-2 tumor cells were hardly stained by the same antibody (g, h).

Table 2 Details on patients' age, sex, tumor location, and annexin A2 staining

Case	Age	Sex	Location	Stainability for annexin A2	
				Perivascular tumor cells	Single invasive tumor cells
1	69	M	L. Temporal	++	−
2	67	M	L. Frontal	++	−
3	76	M	L. Frontal	+++	+
4	58	M	L. Frontal	+	−
5	75	M	L. Temporal	+	−

The results of these proteomic analyses were corroborated by the results of the quantitative RT-PCR and immunohistochemical analyses. Nearly all proteins that were shown to be upregulated by the 2DGE method were also upregulated at the mRNA level. This method is simple, reproducible, and reliable and may prove useful for gaining a broader understanding of invasion in general as well as some of the advantages and pitfalls of other *in vitro* modeling systems.

As a shortcoming, 2DGE analysis usually cannot detect hydrophobic membrane proteins, proteins larger than 100 kDa, low-abundance proteins,[9] or proteins with isoelectric point (pI) values outside the pH range.[10] These limitations of standard 2DGE probably account for fewer opportunities in this study to identify these types of proteins in J3T-1 and J3T-2 cells.

Advantages of the two subclones for proteomic analysis

There are several advantages in using invasive animal models and proteomic analysis to study the molecular basis of glioma invasion.

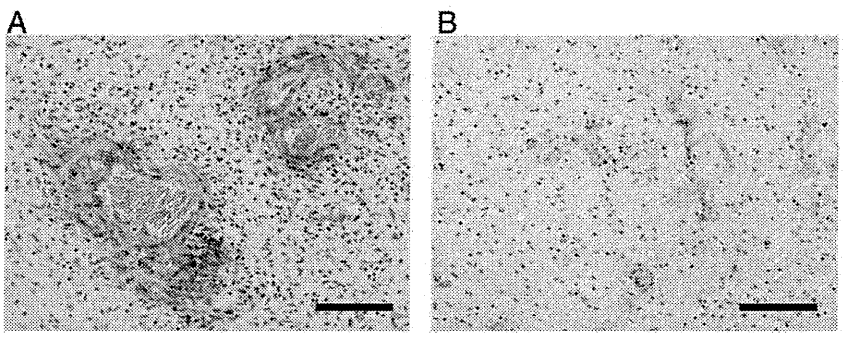

Fig. 5 Results of immunohistochemical analysis of annexin A2 in human glioma samples. Representative photomicrographs of paraffin-embedded sections of glioblastomas from patient 2, which were immunostained for annexin A2. Cells clustering around the dilated vessels located at the border of the tumor are moderately positive for annexin A2 (a). Tumor cells migrating from the tumor center into normal brain parenchyma were mostly negative or very weakly positive for annexin A2 (b). Magnification, ×100. Scale bar = 200 μm.

First, the animal models used in this study are one of the few models available for studying invasive glioma in experimental settings.[1,2] Traditional animal glioma models do not exhibit invasive growth into the surrounding normal brain areas and have been criticized for not recapitulating the main pathological features of human glioma.[11] Recently, several experimental glioma models showing varying degrees of invasion have been developed to study glioma cell invasion both *in vitro* and *in vivo*.[12,13]

Second, the two subclones that were established from the same parental cell line showed very different invasive phenotypes when inoculated in rat brains; however, the subclones have inherently similar genetic backgrounds.[4] These differences in phenotypes are supposed to arise from differences in genotype. This allowed for direct comparison of the differentially expressed proteins that characterize the phenotypic differences in their invasive capabilities.

Third, the animal models used in this study are reproducible and suitable for *in vivo* experiments. Therefore, candidate proteins that might affect the invasive capability of the tumor can be directly verified *in vivo* using these animal models.

Annexin A2 as a candidate invasion-related protein

One of the proteins identified, annexin A2, was expressed at higher levels in J3T-1 cells than in J3T-2 cells. Annexin A2 has been previously reported to be expressed on the tumor cell surface and to be involved in tumor invasion and metastasis.[6–8] Therefore, this protein's role in both animal models and human glioma samples was further examined.

Annexins are a superfamily of closely related calcium- and membrane-binding proteins that are expressed in specific cell types. Annexins comprise numerous gene products, including 12 that are formed in vertebrates (group A annexins) and have been proposed to be involved in a variety of functions, including control of membrane structures, vesicle trafficking, cell division, apoptosis, calcium signaling and growth regulation.[14–20] All annexins share a characteristic molecular structure that consists of a variable N-terminal domain and a highly conserved C-terminal domain, which is also called the annexin core. The core domain of annexin A2 harbors several Ca^{2+}-binding sites and one actin-binding domain, whereas the N-terminal domain contains the binding site for the cellular ligand S100A10 and a Ca^{2+}-independent membrane-binding domain. In cells, annexin A2 exists either as a monomer or as a heterotetrameric complex with S100A10.[21] Cell-surface annexin A2 has been shown to be a receptor/binding protein for both proteases (cathepsin B, plasminogen and tissue-type plasminogen activator (tPA)) and extracellular matrix proteins (type I collagen and tenascin C) that are involved in tumor invasion and metastasis.[6–8] tPA has been shown to bind specifically to annexin A2 on the extracellular membrane of pancreatic cancer cells where it activates plasmin production and promotes tumor cell invasion. Annexin A2 is also expressed on the surface of vascular endothelial cells and has been shown to play a significant role in the regulation of tPA activities, plasminogen activation and angiogenic functions.[22,23] Increased expression of annexin A2 has been described in several types of tumor, including gastric carcinoma,[24] colorectal cancer,[25] pancreatic cancer,[26] breast cancer,[27] high-grade gliomas,[28] kidney cancer[29] and vascular tumors.[30] In gliomas, annexin A2 has been identified more frequently in high-grade gliomas than in low-grade gliomas[10] and is known to be an independent prognostic factor for poor clinical outcomes in patients with gliomas.[28,31] Because of the ability of annexin A2 to interact with the actin cytoskeleton[14,15,32] and tumor-released proteases,[15] annexin A2 has become a promising candidate for influencing the invasion processes of glioma cells. Recent proteomic investigations of the pseudopodia extensions of highly migratory U87MG glioma cells have reported increased levels of annexin A2.[33] Tatenhorst *et al.* demonstrated that the migration of human glioma cells is significantly inhibited following annexin A2 depletion by RNA interference techniques *in vitro*.[34] Moreover, cell-surface annexin A2 is a receptor for angiostatin, which is an internal fragment of plasminogen. Annexin A2-dependent

localized plasmin generation could contribute to angiogenesis and metastasis. Therefore, by blocking annexin A2-dependent plasmin production, for example, by using angiostatin, it may be possible to develop new anti-angiogenic therapies.[35]

A previous study reported that there are at least two invasive and angiogenic phenotypes – angiogenesis-dependent invasion and angiogenesis-independent invasion – and the novel animal glioma models used in this study were able to exhibit these phenotypes.[1,2] The histopathological features of angiogenesis-dependent invasion are characterized by robust neovascular formation in the normal parenchyma adjacent to the main tumor mass and the formation of clusters of glioma cells. In contrast, angiogenesis-independent invasion is characterized by the formation of poorly demarcated tumors that show single-cell infiltrations into the surrounding normal brain tissue without angiogenic activities.

In the present study, annexin A2 was upregulated in J3T-1 cells, which typically show angiogenesis-dependent invasion in the rat brain. In addition, immunohistochemical analysis of human glioblastoma samples revealed that annexin A2 is expressed in clusters of tumor cells around dilated vessels located at the border of the tumor, suggesting that annexin A2 has a functional role in angiogenesis-dependent invasion. The authors consider that neoangiogenesis is an important factor that contributes to the regulation of invasion patterns. Recent studies have shown that glioma cell lines derived from transgenic mice that lack VEGF expression form tumors with irregular borders and are highly invasive along blood vessels, as compared with the sharp borders seen in tumors derived from the glioma cells that have been transfected to overexpress VEGF.[36] This observation is consistent with the result of the present study, suggesting that annexin A2 plays a key role in angiogenesis-dependent invasion by interacting with VEGF and other proangiogenic factors. With regard to the relationship between annexin A2 and VEGF, Zhao *et al.* demonstrated that the increased expression of annexin A2 in ischemic retinas is induced by increased levels of VEGF mRNA. Zhao *et al.* concluded that annexin A2 is a functional protein in VEGF expression in retinal neovascularization and is induced by hypoxia.[37]

Additional findings

Other noticeable proteins expressed higher in J3T-2 are heterogeneous nuclear ribonucleoproteins (hnRNPs) and Septin 11.

hnRNPs comprise a large family of proteins, including approximately 30 members that share some structural domains. The results obtained in our study show heterogeneous nuclear ribonucleoprotein K (HNRNPK) and HNRNPA1 are up-regulated in J3T-2. hnRNPs play important roles in telomere biogenesis, DNA repair, cellular signaling, and the regulation of expression at both the transcriptional and translational levels.[38] In addition, the nuclear shift of HNRNPK in dividing cells suggests a role in proliferating cells.[39] So far, there have been no detailed reports about functions of hnRNPs in gliomas.

Septins are a highly conserved subfamily of GTPases that play an important role in maintaining cytoskeletal structures necessary for the control of cell division, and are required for cytokinesis.[40] Kim *et al.* showed that septins are variably expressed in human brain tumor cell lines and specimens using antibodies against septins 2, 3, 4, 5, 6, 7, 9 and 11 in immunofluorescence and Western blot analysis.[41] In their study, septin 11 was immunolocalized along with the actin microfilamentous system, suggesting possible involvement in cell motility function.

These proteins are not fully investigated in terms of their function in glioma invasion and await further study.

CONCLUSION

Proteomic methods were used to compare the protein profiles of two cell lines with different invasive characteristics. This comparative analysis revealed the differential expression of several proteins that may be involved in tumor cell invasion. Among them, annexin A2 was shown to be one of the candidate proteins which are involved in angiogenesis-dependent invasion.

This study will help to elucidate the mechanisms involved in glioma cell invasion and will aid in the selection of targets for the molecular treatment of malignant gliomas.

ACKNOWLEDGMENTS

This study was supported by grants-in-aid for Scientific Research from the Japanese Ministry of Education, Culture, Sports, Science, and Technology to T.I. (No. 19591675), H.K. (No. 19591676), and K.K. (No. 20890133; no. 21791364), and Okayama University Budget for Centers of Excellence. We thank H. Wakimoto, M. Arao, and A. Ishikawa for their technical assistance. The following medical students also contributed animal experiments: T. Oka, K. Tanaka, H. Honda, K. Seno, H. Okura, T. Mifune, and S. Murai.

REFERENCES

1. Inoue S, Ichikawa T, Kurozumi K *et al.* Novel animal glioma models that separately exhibit two different invasive and angiogenic phenotypes of human glioblastomas. *World Neurosurg* 2012. doi: 10.1016/j.wneu.2011.09.005.

2. Onishi M, Ichikawa T, Kurozumi K, Date I. Angiogenesis and invasion in glioma. *Brain Tumor Pathol* 2011; **28**: 13–24.
3. Berens ME, Bjotvedt G, Levesque DC, Rief MD, Shapiro JR, Coons SW. Tumorigenic, invasive, karyotypic, and immunocytochemical characteristics of clonal cell lines derived from a spontaneous canine anaplastic astrocytoma. *In Vitro Cell Dev Biol Anim* 1993; **29**: 310–318.
4. Hampl JA, Camp SM, Mydlarz WK *et al.* Potentiated gene delivery to tumors using herpes simplex virus/Epstein-Barr virus/RV tribrid amplicon vectors. *Hum Gene Ther* 2003; **14**: 611–626.
5. Ichikawa T, Tamiya T, Adachi Y *et al.* In vivo efficacy and toxicity of 5-fluorocytosine/cytosine deaminase gene therapy for malignant gliomas mediated by adenovirus. *Cancer Gene Ther* 2000; **7**: 74–82.
6. Mai J, Waisman DM, Sloane BF. Cell surface complex of cathepsin B/annexin II tetramer in malignant progression. *Biochim Biophys Acta* 2000; **1477**: 215–230.
7. Díaz VM, Hurtado M, Thomson TM, Reventós J, Paciucci R. Specific interaction of tissue-type plasminogen activator (t-PA) with annexin II on the membrane of pancreatic cancer cells activates plasminogen and promotes invasion in vitro. *Gut* 2004; **53**: 993–1000.
8. Zhai H, Acharya S, Gravanis I *et al.* Annexin A2 promotes glioma cell invasion and tumor progression. *J Neurosci* 2011; **31**: 14346–14360.
9. Vogel TW, Zhuang Z, Li J *et al.* Proteins and protein pattern differences between glioma cell lines and glioblastoma multiforme. *Clin Cancer Res* 2005; **11**: 3624–3632.
10. Iwadate Y, Sakaida T, Hiwasa T *et al.* Molecular classification and survival prediction in human gliomas based on proteome analysis. *Cancer Res* 2004; **64**: 2496–2501.
11. de Vries NA, Beijnen JH, van Tellingen O. High-grade glioma mouse models and their applicability for preclinical testing. *Cancer Treat Rev* 2009; **35**: 714–723.
12. Martens T, Laabs Y, Günther HS *et al.* Inhibition of glioblastoma growth in a highly invasive nude mouse model can be achieved by targeting epidermal growth factor receptor but not vascular endothelial growth factor receptor-2. *Clin Cancer Res* 2008; **14**: 5447–5458.
13. Giannini C, Sarkaria JN, Saito A *et al.* Patient tumor EGFR and PDGFRA gene amplifications retained in an invasive intracranial xenograft model of glioblastoma multiforme. *Neuro Oncol* 2005; **7**: 164–176.
14. Rescher U, Gerke V. Annexins–unique membrane binding proteins with diverse functions. *J Cell Sci* 2004; **117**: 2631–2639.
15. Gerke V, Moss SE. Annexins: from structure to function. *Physiol Rev* 2002; **82**: 331–371.
16. Gerke V, Creutz CE, Moss SE. Annexins: linking Ca2+ signalling to membrane dynamics. *Nat Rev Mol Cell Biol* 2005; **6**: 449–461.
17. Hayes MJ, Moss SE. Annexins and disease. *Biochem Biophys Res Commun* 2004; **322**: 1166–1170.
18. Hayes MJ, Longbottom RE, Evans MA, Moss SE. Annexinopathies. *Subcell Biochem* 2007; **45**: 1–28.
19. Rand JH. The annexinopathies: a new category of diseases. *Biochim Biophys Acta* 2000; **1498**: 169–173.
20. Mussunoor S, Murray GI. The role of annexins in tumour development and progression. *J Pathol* 2008; **216**: 131–140.
21. Zobiack N, Gerke V, Rescher U. Complex formation and submembranous localization of annexin 2 and S100A10 in live HepG2 cells. *FEBS Lett* 2001; **500**: 137–140.
22. Ling Q, Jacovina AT, Deora A *et al.* Annexin II regulates fibrin homeostasis and neoangiogenesis in vivo. *J Clin Invest* 2004; **113**: 38–48.
23. Hajjar KA, Jacovina AT, Chacko J. An endothelial cell receptor for plasminogen/tissue plasminogen activator. I. Identity with annexin II. *J Biol Chem* 1994; **269**: 21191–21197.
24. Emoto K, Sawada H, Yamada Y *et al.* Annexin II overexpression is correlated with poor prognosis in human gastric carcinoma. *Anticancer Res* 2001; **21**: 1339–1345.
25. Duncan R, Carpenter B, Main LC, Telfer C, Murray GI. Characterization and protein expression profiling of annexins in colorectal cancer. *Br J Cancer* 2008; **98**: 426–433.
26. Esposito I, Penzel R, Chaib-Harrireche M *et al.* Tenascin C and annexin II expression in the process of pancreatic carcinogenesis. *J Pathol* 2006; **208**: 673–685.
27. Sharma MR, Koltowski L, Ownbey RT, Tuszynski GP, Sharma MC. Angiogenesis-associated protein annexin II in breast cancer: selective expression in invasive breast cancer and contribution to tumor invasion and progression. *Exp Mol Pathol* 2006; **81**: 146–156.
28. Reeves SA, Chavez-Kappel C, Davis R, Rosenblum M, Israel MA. Developmental regulation of annexin II (Lipocortin 2) in human brain and expression in high grade glioma. *Cancer Res* 1992; **52**: 6871–6876.
29. Zimmermann U, Woenckhaus C, Pietschmann S *et al.* Expression of annexin II in conventional renal cell carcinoma is correlated with Fuhrman grade and clinical outcome. *Virchows Arch* 2004; **445**: 368–374.
30. Syed SP, Martin AM, Haupt HM, Arenas-Elliot CP, Brooks JJ. Angiostatin receptor annexin II in vascular tumors including angiosarcoma. *Hum Pathol* 2007; **38**: 508–513.
31. Siao CJ, Tsirka SE. Tissue plasminogen activator mediates microglial activation via its finger domain through annexin II. *J Neurosci* 2002; **22**: 3352–3358.

32. Hayes MJ, Rescher U, Gerke V, Moss SE. Annexin-actin interactions. *Traffic* 2004; **5**: 571–576.
33. Beckner ME, Chen X, An J, Day BW, Pollack IF. Proteomic characterization of harvested pseudopodia with differential gel electrophoresis and specific antibodies. *Lab Invest* 2005; **85**: 316–327.
34. Tatenhorst L, Rescher U, Gerke V, Paulus W. Knockdown of annexin 2 decreases migration of human glioma cells in vitro. *Neuropathol Appl Neurobiol* 2006; **32**: 271–277.
35. Sharma MC, Sharma M. The role of annexin II in angiogenesis and tumor progression: a potential therapeutic target. *Curr Pharm Des* 2007; **13**: 3568–3575.
36. Pàez-Ribes M, Allen E, Hudock J *et al.* Antiangiogenic therapy elicits malignant progression of tumors to increased local invasion and distant metastasis. *Cancer Cell* 2009; **15**: 220–231.
37. Zhao S, Huang L, Wu J, Zhang Y, Pan D, Liu X. Vascular endothelial growth factor upregulates expression of annexin A2 in vitro and in a mouse model of ischemic retinopathy. *Mol Vis* 2009; **15**: 1231–1242.
38. Carpenter B, MacKay C, Alnabulsi A *et al.* The roles of heterogeneous nuclear ribonucleoproteins in tumour development and progression. *Biochim Biophys Acta* 2006; **1765**: 85–100.
39. Ostrowski J, Bomsztyk K. Nuclear shift of hnRNP K protein in neoplasms and other states of enhanced cell proliferation. *Br J Cancer* 2003; **89**: 1493–1501.
40. Kinoshita M, Kumar S, Mizoguchi A *et al.* Nedd5, a mammalian septin, is a novel cytoskeletal component interacting with actin-based structures. *Genes Dev* 1997; **11**: 1535–1547.
41. Kim DS, Hubbard SL, Peraud A, Salhia B, Sakai K, Rutka JT. Analysis of mammalian septin expression in human malignant brain tumors. *Neoplasia* 2004; **6**: 168–178.

Neurology & Neurophysiology

Moriuchi et al., J Neurol Neurophysiol 2013, 4:3
http://dx.doi.org/10.4172/2155-9562.1000159

Research Article Open Access

Use of 5-Aminolevulinic Acid to Detect Residual Meningioma and Ensure Total Removal while Avoiding Neurological Deficits

Shusuke Moriuchi[1*], Kimito Yamada[1], Makoto Dehara[1], Yoshifumi Teramoto[1], Takao Soda[2], Masami Imakita[3], Mamoru Taneda[1]

[1]Departments of Neurosurgery, Rinnku General Medical Center, Izumisano, Osaka, Japan
[2]Departments of Neurology, Rinnku General Medical Center, Izumisano, Osaka, Japan
[3]Departments of 3Pathology, Rinnku General Medical Center, Izumisano, Osaka, Japan

Abstract

5-Aminolevulinic acid (5-ALA) has been used successfully to resect meningioma without leaving a residual mass. The authors report their experience resecting meningiomas in 17 patients using 5-ALA. Except for one case, all meningiomas fluoresced intra-operatively under the microscope. Invasion to the dura mater, brain parenchyma, or skull showed fluorescence, allowing for confirmation of residual tumor; total removal of the meningioma could be performed more easily, and unexpected neurological deficits could be prevented by precise removal of the tumor under the microscope. With invasion to the dura mater or skull in one case, the extent of dural removal was decided by 5-ALA fluorescence with 1- to 2-cm safety margins. In another case with parenchymal invasion, close removal of the tumor without leaving residual tumor could be performed with 5-ALA fluorescence. With the above methods, no serious side effects or complications occurred in this study. Not all meningiomas fluoresced with 5-ALA, and 5-ALA is available for about 95% of meningiomas. 5-ALA appears easy to use and helpful for finding residual tumor and preventing recurrences by total removal of meningiomas.

Keywords: 5-ALA; Meningioma; Total resection

Introduction

Complete resection of meningiomas provides patients with the best chance for a cure; however, surgery is frequently difficult given the proximity of lesions to vital structures, such as cranial nerves, major vessels, and venous sinuses [1]. Accurate discrimination between tumor and normal tissue is crucial for optimal tumor resection. With the use of 5-aminolevulinic acid (ALA), meningiomas can be seen to fluoresce intra-operatively under the microscope [2]. Invasion to the dura mater, brain parenchyma, or skull shows fluorescence, allowing for confirmation of residual tumor, and total removal of the meningioma could be performed more easily, while unexpected neurological deficits could be prevented by precise removal of the tumor under the microscope. In the past 2 years, 17 total resections of meningiomas were performed using 5-ALA without recurrences and major complications, and it was found that fluorescence-guided resection may be beneficial for removal of complicated meningiomas that have a high risk of recurrence.

Methods

Patients' characteristics

A total of 17 consecutive patients (16 females, 1 male; average age, 65.5 years) undergoing resection of intracranial meningiomas from January 2011 to December 2012 were included in this study (Table 1). All of the meningiomas were histologically Grade I meningiomas. Tumor locations varied and included parasagittal, falx, sphenoid ridge, convexity, planum sphenoidale, and petroclival tumors. The sizes of the meningiomas ranged from more than 21 mm in diameter (Case 7) to a maximum of 76 mm in diameter (Case 2). In 4 of 17 cases, the middle meningeal artery feeding the meningioma was embolized preoperatively.

Preoperative and intraoperative procedures

After confirmation of normal liver function, patients were given 20 mg/kg of 5-ALA (Cosmo Oil Co., Ltd., Japan) 4 hours preoperatively [2,3]. Craniotomies were performed under general anesthesia. The meningiomas were confirmed using a 440-nm ultraviolet light source (violet-blue light), an optical component of the OPMI Pentero microscope (Carl Zeiss AG, Germany). Under the violet-blue light, the meningiomas showed charcoal-red fluorescence. Total removal of the meningiomas could be performed by resecting the tumor until the charcoal-red fluorescence could no longer be detected. In cases of proximity to vital organs, it is important to prevent damage to these organs and carefully remove the charcoal-red residual tumors.

Results

Tumor fluorescence

All 17 tumors were totally resected using 5-ALA fluorescence. No major neurological deficits were observed after surgery. The histopathological diagnosis of these 17 meningiomas was WHO grade 1 meningioma; the tumors' MIB-1 indices did not reach 5%. At the latest follow-up examination, 2 years after surgery, no patients showed evidence of recurrence. In 4 cases, the middle meningeal artery was embolized preoperatively. Even when the main feeding artery, the middle meningeal artery, was embolized, tumor fluorescence was strong in all cases. No correlation between preoperative embolization and tumor fluorescence was observed. Two cases (Case 4 and Case 5) showed weak tumor fluorescence. In Case 4, the tumor had intratumoral hemorrhage. The histopathological diagnoses were meningothelial meningioma with a MIB-1 index of 2% in Case 4 and transitional meningioma with a

***Corresponding author:** Dr. Shusuke Moriuchi, Departments of Neurosurgery, Rinnku General Medical Center, Izumisano, Osaka, Japan, Tel: 81-72-469-3111; Fax: 81-72-469-7929; E-mail: s-moriuchi@rgmc.izumisano.osaka.jp

Received June 21, 2013; **Accepted** July 29, 2013; **Published** August 05, 2013

Citation: Moriuchi S, Yamada K, Dehara M, Teramoto Y, Soda T, et al. (2013) Use of 5-Aminolevulinic Acid to Detect Residual Meningioma and Ensure Total Removal while Avoiding Neurological Deficits. J Neurol Neurophysiol 4: 159. doi:10.4172/2155-9562.1000159